CompRess: Self-Supervised Learning by Compressing Representations

Soroush Abbasi Koohpayegani* Ajinkya Tejankar* Hamed Pirsiavash

University of Maryland, Baltimore County {soroush, at6, hpirsiav}@umbc.edu

Abstract

Self-supervised learning aims to learn good representations with unlabeled data. Recent works have shown that larger models benefit more from self-supervised learning than smaller models. As a result, the gap between supervised and self-supervised learning has been greatly reduced for larger models. In this work, instead of designing a new pseudo task for self-supervised learning, we develop a model compression method to compress an already learned, deep self-supervised model (teacher) to a smaller one (student). We train the student model so that it mimics the relative similarity between the datapoints in the teacher's embedding space. For AlexNet, our method outperforms all previous methods including the fully supervised model on ImageNet linear evaluation (59.0% compared to 56.5%) and on nearest neighbor evaluation (50.7% compared to 41.4%). To the best of our knowledge, this is the first time a self-supervised AlexNet has outperformed supervised one on ImageNet classification. Our code is available here: https://github.com/UMBCvision/CompRess

1 Introduction

Supervised deep learning needs lots of annotated data, but the annotation process is particularly expensive in some domains like medical images. Moreover, the process is prone to human bias and may also result in ambiguous annotations. Hence, we are interested in self-supervised learning (SSL) where we learn rich representations from unlabeled data. One may use these learned features along with a simple linear classifier to build a recognition system with small annotated data. It is shown that SSL models trained on ImageNet without labels outperform the supervised models when transferred to other tasks [9, 24].

Some recent self-supervised learning algorithms have shown that increasing the capacity of the architecture results in much better representations. For instance, for SimCLR method [9], the gap between supervised and self-supervised is much smaller for ResNet-50x4 compared to ResNet-50 (also shown in Figure 1). Given this observation, we are interested in learning better representations for small models by compressing a deep self-supervised model.

In edge computing applications, we prefer to run the model (e.g., an image classifier) on the device (e.g., IoT) rather than sending the images to the cloud. During inference, this reduces the privacy concerns, latency, power usage, and cost. Hence, there is need for rich, small models. Compressing SSL models goes beyond that and reduces the privacy concerns at the training time as well. For instance, one can download a rich self-supervised MobileNet model that can generalize well to other tasks and finetune it on his/her own data without sending any data to the cloud for training.

Since we assume our teacher has not seen any labels, its output is an embedding rather than a probability distribution over some categories. Hence, standard model distillation methods [26] cannot

^{*}Equal contribution

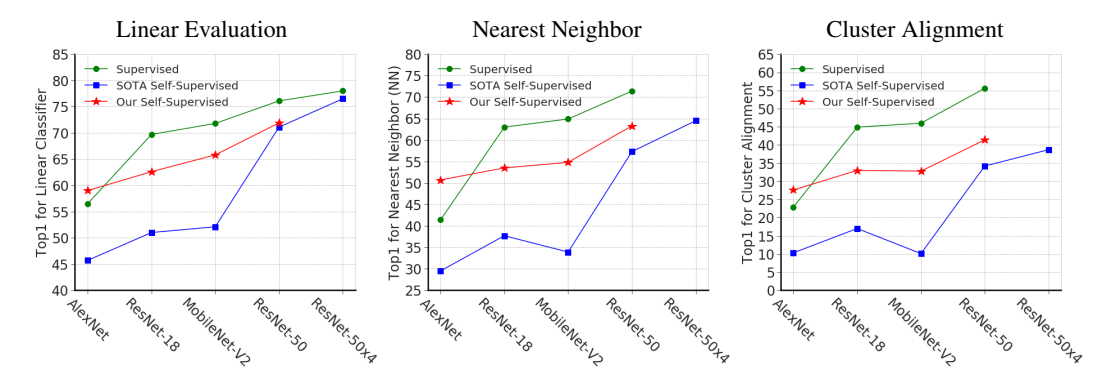


Figure 1: **ImageNet Evaluation:** We compare "Ours-1q" self-supervised model with supervised and SOTA self-supervised models on ImageNet using linear classification (left), nearest neighbor (middle) and cluster alignment (right) evaluations. Our AlexNet model outperforms the supervised counterpart on all evaluations. This model is compressed from ResNet-50x4 trained with SimCLR method using unlabeled ImageNet. All models have seen ImageNet images only. All SOTA SSL models are MoCo except ResNet50x4 that is SimCLR. The teacher for our AlexNet and ResNet50 is SimCLR ResNet50x4 and for ResNet18 and MobileNet-V2 is MoCo ResNet50.

be used directly. One can employ a nearest neighbor classifier in the teacher space by calculating distances between an input image (query) and all datapoints (anchor points) and then converting them to probability distribution. Our idea is to transfer this probability distribution from the teacher to the student so that for any query point, the student matches the teacher in the ranking of anchor points.

Traditionally, most SSL methods are evaluated by learning a linear classifier on the features to perform a downstream task (e.g., ImageNet classification). However, this evaluation process is expensive and has many hyperparameters (e.g., learning rate schedule) that need to be tuned as one set of parameters may not be optimal for all SSL methods. We believe a simple nearest neighbor classifier, used in some recent works [57, 67, 60], is a better alternative as it has no parameters, is much faster to evaluate, and still measures the quality of features. Hence, we use this evaluation extensively in our experiments. Moreover, inspired by [30], we use another related evaluation by measuring the alignment between k-means clusters and image categories.

Our extensive experiments show that our compressed SSL models outperform state-of-the-art compression methods as well as state-of-the-art SSL counterparts using the same architecture on most downstream tasks. Our AlexNet model, compressed from ResNet-50x4 trained with SimCLR method, outperforms standard supervised AlexNet model on linear evaluation (by 2 point), in nearest neighbor (by 9 points), and in cluster alignment evaluation (by 4 points). This is interesting as all parameters of the supervised model are already trained on the downstream task itself but the SSL model and its teacher have seen only ImageNet without labels. To the best of our knowledge, this is the first time an SSL model performs better than the supervised one on the ImageNet task itself instead of transfer learning settings.

2 Related work

Self-supervised learning: In self-supervised learning for images, we learn rich features by solving a pretext task that needs unlabeled data only. The pseudo task may be colorization [64], inpainting [42], solving Jigsaw puzzles [36], counting visual primitives [37], and clustering images [7].

Contrastive learning: Our method is related to contrastive learning [23, 39, 27, 67, 4, 49, 25] where the model learns to contrast between the positive and lots of negative pairs. The positive pair is from the same image and model but different augmentations in [24, 9, 51] and from the same image and augmentation but different models (teacher and student) in [50]. Our method uses soft probability distribution instead of positive/negative classification [67], and does not couple the two embeddings (teacher and student) directly [50] in "Ours-2q" variant. Contrastive learning is improved with a more robust memory bank in [24] and with temperature and better image augmentations in [9]. Our ideas are related to exemplar CNNs [15, 34], but used for compression.

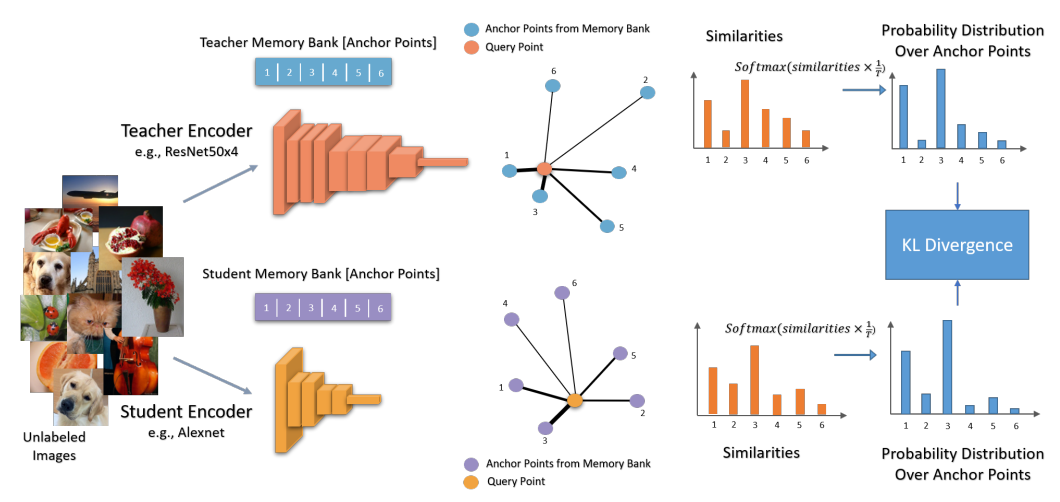


Figure 2: **Our compression method:** The goal is to transfer the knowledge from the self-supervised teacher to the student. For each image, we compare it with a random set of data points called anchors and obtain a set of similarities. These similarities are then converted into a probability distribution over the anchors. This distribution represents each image in terms of its nearest neighbors. Since we want to transfer this knowledge to the student, we get the same distribution from the student as well. Finally, we train the student to minimize the KL divergence between the two distributions. Intuitively, we want each data point to have the same neighbors in both teacher and student embeddings. This illustrates Ours-2q method. For Ours-1q, we simply remove the student memory bank and use the teacher's anchor points for the student as well.

Model compression: The task of training a simpler student to mimic the output of a complex teacher is called model compression in [6] and knowledge distillation in [26]. In [26], the softened class probabilities from the teacher are transferred to the student by reducing KL divergence. The knowledge in the hidden activations of intermediate layers of the teacher is transferred by regressing linear projections [45], aggregation of feature maps [62], and gram matrices [59]. Also, knowledge at the final layer can be transferred in different ways [3, 26, 31, 41, 43, 40, 53, 2, 50, 61, 56, 5, 18, 48]. In [2, 50] distillation is formulated as maximization of information between teacher and student.

Similarity-based distilation: Pairwise similarity based knowledge distillation has been used along with supervised teachers. [43, 53, 40] use supervised loss in distillation. [41] is probably the closest to our setting which does not use labels in the distillation step. We are different as we use memory bank and SoftMax along with temperature, and also apply that to compressing self-supervised models in large scale. We compare with a reproduced variant of [41] in the experiments (Section 4.3).

Model compression for self-supervision: Standard model compression techniques either directly use the output of supervised training [26] or have a supervised loss term [50, 40] in addition to the compression loss term. Thus, they cannot be directly applied to compress self-supervised models. In [38], the knowledge from the teacher is transferred to the student by first clustering the embeddings from teacher and then training the student to predict the cluster assignments. In [58], the method of [38] is applied to regularize self-supervised models.

3 Method

Our goal is to train a deep model (e.g. ResNet-50) using an off-the-shelf self-supervised learning algorithm and then, compress it to a less deep model (e.g., AlexNet) while preserving the disctiminative power of the features.

Assuming a frozen teacher embedding $t(x) \in R^N$ with parameters θ_t that maps an image x into an N-D feature space, we want to learn the student embedding $s(x) \in R^M$ with parameters θ_s that mimics the same behavior as t(x) if used for a downstream supervised task e.g., image classification. Note that the teacher and student may use architectures from different families, so we do not necessarily want to couple them together directly. Hence, we transfer the similarity between data points from the teacher to the student rather than their final prediction.

For simplicity, we use $t_i = t(x_i)$ for the embedding of the model t(x) on the input image x_i normalized by ℓ_2 norm. We assume a random set of the training data $\{x_j\}_{j=1}^n$ are the *anchor* points and embed them using both teacher and student models to get $\{t_j^a\}_{j=1}^n$ and $\{s_j^a\}_{j=1}^n$. Given a *query* image q_i and its embeddings t_i^q for teacher and s_i^q for student, we calculate the pairwise similarity between t_i^q and all anchor embeddings $\{t_j^a\}_{j=1}^n$, and then optimize the student model so that in the student's embedding space, the query s_i^q has the same relationship with the anchor points $\{s_j^a\}_{j=1}^n$.

To measure the relationship between the query and anchor points, we calculate their cosine similarity. We convert the similarities to the form of a probability distribution over the anchor points using SoftMax operator. For the teacher, the probability of the i-th query for the j-th anchor point is:

$$p_{j}^{i}(t) = \frac{\exp(t_{i}^{qT} t_{j}^{a} / \tau)}{\sum_{k=1}^{n} \exp(t_{i}^{qT} t_{k}^{a} / \tau)}$$

where τ is the temperature hyperparamater. Then, we define the loss for a particular query point as the KL divergence between the probabilities over all anchor points under the teacher and student models, and we sum this loss over all query points:

$$L(t,s) = \sum_{i} KL(p^{i}(t)||p^{i}(s))$$

where $p^i(s)$ is the probability distribution of query i over all anchor points on the student network. Finally, since the teacher is frozen, we optimize the student by solving:

$$\mathop{\arg\min}_{\theta_s} L(t,s) = \mathop{\arg\min}_{\theta_s} \sum_{i,j} -p^i_j(t).log(p^i_j(s))$$

Memory bank: One may use the same minibatch for both query and anchor points by excluding the query from each set of anchor points. However, we need a large set of anchor points (ideally the whole training set) so that they have large variation to cover the neighborhood of any query image. Our experiments verify that using the minibatch of size 256 for anchor points is not enough for learning rich representations. This is reasonable as ImageNet has 1000 categories so the query may not be close to any anchor point in a minibatch of size 256. However, it is computationally expensive to process many images in a single iteration due to limited computation and memory. Similar to [57], we maintain a memory bank of anchor points from several most recent iterations. We use momentum contrast [24] framework for implementing memory bank for the student. However, unlike [24], we find that our method is not affected by the momentum parameter which requires further investigation. Since the teacher is frozen, we implement its memory bank as a simple FIFO queue.

Temperature parameter: Since the anchor points have large variation covering the whole dataset, many of them may be very far from the query image. We use a small temperature value (less than one) since we want to focus mainly on transferring the relationships from the close neighborhoods of the query rather than faraway points. Note that this results in sharper probabilities compared to $\tau=1$. We show that $\tau=1$ degrades the results dramatically. The temperature value acts similarly to the kernel width in kernel density estimation methods.

Student using teacher's memory bank: So far, we assumed that the teacher and student embeddings are decoupled, so used a separate memory bank (queue) for each. We call this method **Ours-2q**. However, we may use the teacher's anchor points in calculating the similarity for the student model. This way, the model may learn faster and be more stable in the initial stages of learning, since the teacher anchor points are already mature. We call this variation **Ours-1q** in our experiments. Note that in "Ours-1q" method, we do not use momentum since the teacher is constant.

Caching the teacher embeddings: Since we are interested in using very deep models (e.g., ResNet-50x4) as the teacher, calculating the embeddings for the teacher is expensive in terms of both computation and memory. Also, we are not optimizing the teacher model. Hence, for such large models, we can cache the results of the teacher on all images of the dataset and keep them in the memory. This caching has a drawback that we cannot augment the images for the teacher, meaning that the teacher sees exact same images in all epochs. However, since the student still sees augmented images, it is less prone to overfitting. On the other hand, this caching may actually help the student by encouraging the relationship between the query and anchor points to be close even under different augmentations, hence, improving the representation in a way similar to regular contrastive learning

[57, 24]. In our experiments, we realize that caching degrades the results by only a small margin while is much faster and efficient in learning. We use caching when we compress from ResNet-50x4 to AlexNet.

4 Experiments and results

We use different combinations of architectures as student-teacher pairs (listed in Table 1). We use three teachers: (a) ResNet-50 model which is trained using MoCo-v2 method for 800 epochs [10], (b) ResNet-50 trained with SwAV [8] for 800 epochs, and (c) ResNet-50x4 model which is trained using SimCLR method for 1000 epochs [9]. We use the officially published weights of these models [44, 47, 54]. For supervised models, we use the official PyTorch weights [52]. We use ImageNet (ILSVRC2012) [46] without labels for all self-supervised and compression methods, and use various datasets (ImageNet, PASCAL-VOC [16], Places [66], CUB200 [55], and Cars196 [32]) for evaluation.

Implementation details: Here, we report the implementation details for Ours-2q and Ours-1q compression methods. The implementation details for all baselines and transfer experiments are included in the appendix. We use PyTorch along with SGD (weight decay=1e-4, learning rate=0.01, momentum=0.9, epochs=130, and batch size=256). We multiply learning rate by 0.2 at epochs 90 and 120. We use standard ImageNet data augmentation found in PyTorch. Compressing from ResNet-50x4 to ResNet-50 takes ~100 hours on four Titan-RTX GPUs while compressing from ResNet-50 to ResNet-18 takes ~90 hours on two 2080-TI GPUs. We adapt the unofficial implementation of MoCo [24] in [11] to implement memory bank for our method. We use memory bank size of 128,000 and set moving average weight for key encoder to 0.999. We use the temperature of 0.04 for all experiments involving SimCLR ResNet-50x4 and MoCo ResNet-50 teachers. We pick these values based on the ablation study done for the temperature parameter in Section 4.5. For SwAV ResNet-50 teacher, we use a temperature of 0.007 since we find that it works better than 0.04.

4.1 Evaluation Metrics

Linear classifier (Linear): We treat the student as a frozen feature extractor and train a linear classifier on the labeled training set of ImageNet and evaluate it on the validation set with Top-1 accuracy. To reduce the computational overhead of tuning the hyperparameters per experiment, we standardize the Linear evaluation as following. We first normalize the features by ℓ_2 norm, then shift and scale each dimension to have zero mean and unit variance. For all linear layer experiments, we use SGD with lr=0.01, epochs=40, batch size=256, weight decay=1e-4, and momentum=0.9. At epochs 15 and 30, the lr is multiplied by 0.1.

Nearest Neighbor (NN): We also evaluate the student representations using nearest neighbor classifier with cosine similarity. We use FAISS GPU library [1] to implement it. This method does not need any parameter tuning and is very fast (~25 minutes for ResNet-50 on a single 2080-TI GPU)

Cluster Alignment (CA): The goal is to measure the alignment between clusters of our SSL representations with visual categories, e.g., ImageNet categories. We use k-means (with k=1000) to cluster our self-supervised features trained on unlabeled ImageNet, map each cluster to an ImageNet category, and then evaluate on ImageNet validation set. In order to map clusters to categories, we first calculate the alignment between all (cluster- category) pairs by calculating the number of common images divided by the size of cluster. Then, we find the best mapping between clusters and categories using Hungarian algorithm [33] that maximizes total alignment. This labels the clusters. Then, we report the classification accuracy on the validation set. This setting is similar to the object discovery setting in [30]. In Figure 3 (c), we show some random images from random clusters where images inside each cluster are semantically related.

4.2 Baselines:

Contrastive Representation Distillation (CRD): CRD [50] is an information maximization based SOTA method for distillation that includes a supervised loss term. It directly compares the embeddings of teacher and student as in a contrastive setting. We remove the supervised loss in our experiments.

Cluster Classification (CC): Cluster Classification [38] is an unsupervised knowledge distillation method that improves self-supervised learning by quantizing the teacher representations. This is similar to the recent work of ClusterFit [58].

Table 1: Comparison of distillation methods on full ImageNet: Our method is better than all compression methods for various teacher-student combinations and evaluation benchmarks. In addition, as reported in Table 5 and Figure 1, when we compress ResNet-50x4 to AlexNet, we get 59.0% for Linear, 50.7% for Nearest Neighbor (NN), and 27.6% for Cluster Alignment (CA) which outperforms the supervised model. On NN, our ResNet-50 is only 1 point worse than its ResNet-50x4 teacher. Note that models below the teacher row use the student architecture. Since a forward pass through the teacher is expensive for ResNet50x4, we do not compare with CRD, Reg, and Reg-BN.

Teacher Student		ResNe lexNet			ResNe sNet-1			ResNe ileNet-			Net-50x sNet-50	
	Linear	NN	CA	Linear	NN	CA	Linear	NN	CA	Linear	NN	CA
Teacher	70.8	57.3	34.2	70.8	57.3	34.2	70.8	57.3	34.2	75.6	64.5	38.7
Supervised	56.5	41.4	22.9	69.8	63.0	44.9	71.9	64.9	46.0	76.2	71.4	55.6
CC [38]	46.4	31.6	13.7	61.1	51.1	25.2	59.2	50.2	24.7	68.9	55.6	26.4
CRD [50]	54.4	36.9	14.1	58.4	43.7	17.4	54.1	36.0	12.0	-	-	-
Reg	49.9	35.6	9.5	52.2	41.7	25.6	48.0	38.6	25.4	_	-	-
Reg-BN	56.1	42.8	22.3	58.2	47.3	27.2	62.3	48.7	27.0	_	-	-
Ours-2q	56.4	48.4	33.3	61.7	53.4	34.7	63.0	54.4	35.5	71.0	63.0	41.1
Ours-1q	57.5	48.0	27.0	62.6	53.5	33.0	65.8	54.8	32.8	71.9	63.3	41.4

Table 2: Comparison of distillation methods on full ImageNet for SwAV ResNet-50 (teacher) to ResNet-18 (student):. Note that SwAV (concurrent work) [8] is different from MoCo and SimCLR in that it performs contrastive learning through online clustering.

	le report NN eval		
	g small training d		
•	Net-18 compresse		
ResNet-50. For	1-shot, we report	t the s	tandard
deviation over 1	0 runs.		
Model	1-shot	1%	10%

Table 3: NN evaluation for ImageNet with

Method	Linear	NN	CA
Teacher	75.6	60.7	27.6
Supervised	69.8	63.0	44.9
CRD	58.2	44.7	16.9
CC	60.8	51.0	22.8
Reg-BN	60.6	47.6	20.8
Ours-2q	62.4	53.7	26.7
Ours-1q	65.6	56.0	26.3

Model	1-shot	1%	10%
Supervised (entire labeled ImageNet)	29.8 (± 0.3)	48.5	56.8
CC [38] CRD [50] Reg-BN Ours-2q	16.3 (\pm 0.3) 11.4 (\pm 0.3) 21.5 (\pm 0.1) 29.0 (\pm 0.3)	31.6 23.3 33.4 41.2	41.9 33.6 40.1 47.6
Ours-1q	$26.5 \ (\pm 0.3)$	39.6	47.2

Regression (**Reg**): We implement a modified version of [45] that regresses only the embedding layer features [61]. Similar to [45, 61], we add a linear projection head on top of the student to match the embedding dimension of the teacher. As noted in CRD [50], transferring knowledge from all intermediate layers does not perform well since the teacher and student may have different architecture styles. Hence, we use the regression loss only for the embedding layer of the networks.

Regression with BatchNorm (Reg-BN): We realized that Reg does not perform well for model compression. We suspect the reason is the mismatch between the embedding spaces of the teacher and student networks. Hence, we added a non-parametric Batch Normalization layer for the last layer of both student and teacher networks to match their statistics. The BN layer uses statistics from the current minibatch only (element-wise whitening). Interestingly, this simple modified baseline is better than other sophisticated baselines for model compression.

4.3 Experiments Comparing Compression Methods

Evaluation on full ImageNet: We train the teacher on unlabeled ImageNet, compress it to the student, and evaluate the student using ImageNet validation set. As shown in Table 1, our method outperforms other distillation methods on all evaluation benchmarks. For a fair comparison, on ResNet-18, we trained MoCo for 1,000 epochs and got 54.5% in Linear and 41.1% in NN which does not still match our model. Also, a variation of our method (MoCo R50 to R18) without *SoftMax*,

Table 4: **Transfer to CUB200 and Cars196:** We train the features on unlabeled ImageNet, freeze the features, and return top k nearest neighbors based on cosine similarity. We evaluate the recall at different k values (1, 2, 4, and 8) on the validation set.

Method			CUE	3200			Cars	s196	
AlexNet	Teacher	R@1	R@2	R@4	R@8	R@1	R@2	R@4	R@8
Sup. on ImageNet	-	33.5	45.5	59.2	71.9	26.6	36.3	45.9	57.8
CRD [50]	ResNet-50	16.6	25.9	36.3	48.7	20.9	28.2	37.7	48.9
Reg-BN	ResNet-50	16.8	25.5	36.2	48.0	20.9	29.0	38.5	49.7
CC	ResNet-50	23.2	32.5	45.1	58.2	23.7	31.4	41.1	52.4
Ours-2q	ResNet-50	23.1	33.0	45.1	58.0	23.6	32.8	42.9	54.9
Ours-1q	ResNet-50	22.7	31.9	43.2	55.8	22.5	30.6	40.4	52.3
CC	ResNet-50x4	23.6	33.6	44.9	58.4	25.4	33.2	43.2	54.3
Ours-2q	ResNet-50x4	26.5	37.0	49.4	62.4	28.4	38.5	48.7	60.4
Ours-1q	ResNet-50x4	21.9	32.4	43.2	55.9	25.0	34.2	45.1	57.3

temperature, and memory bank (similar to [41]) results in 53.6% in Linear and 42.3% in NN. To evaluate the effect of the teacher's SSL method, in Table 2, we use SwAV ResNet-50 as the teacher and compress it to ResNet-18. We still get better accuracy compared to other distillation methods.

Evaluation on smaller ImageNet: We evaluate our representations by a NN classifier using only 1%, 10%, and only 1 sample per category of ImageNet. The results are shown in Table 3. For 1-shot, "Ours-2q" model achieves an accuracy close to the supervised model which has seen all labels of ImageNet in learning the features.

Transfer to CUB200 and Cars196: We transfer AlexNet student models to the task of image retrieval on CUB200 [55] and Cars196 [32] datasets. We evaluate on these tasks without any fine-tuning. The results are shown in Table 4. Surprisingly, for the combination of Cars196 dataset and ResNet-50x4 teacher, our model even outperforms the ImageNet supervised model. Since in "Ours-2q", the student embedding is less restricted and does not follow the teacher closely, the student may generalize better compared to "Ours-1q" method. Hence, we see better results for "Ours-2q" on almost all transfer experiments. This effect is similar to [38, 58].

4.4 Experiments Comparing Self-Supervised Methods

Evaluation on ImageNet: We compare our features with SOTA self-supervised learning methods on Table 5 and Figure 1. Our method outperforms all baselines on all small capacity architectures (AlexNet, MobileNet-V2, and ResNet-18). On AlexNet, it outperforms even the supervised model. Table 6 shows the results of linear classifier using only 1% and 10% of ImageNet for ResNet-50.

Transferring to Places: We evaluate our intermediate representations learned from unlabeled ImageNet on Places scene recognition task. We train linear layers on top of intermediate representations similar to [21]. Details are in the appendix. The results are shown in Table 5. We find that our best layer performance is better than that of a model trained with ImageNet labels.

Transferring to PASCAL-VOC: We evaluate AlexNet compressed from ResNet-50x4 on PASCAL-VOC classification and detection tasks in Table 7. For classification task, we only train a linear classifier on top of frozen backbone which is in contrast to the baselines that finetune all layers. For object detection, we use the Fast-RCNN [20] as used in [38, 19] to finetune all layers.

4.5 Ablation Study

To speed up the ablation study, we use 25% of ImageNet (randomly sampled ~320k images) and cached features of MoCo ResNet-50 as a teacher to train ResNet-18 student. For temperature ablation study, the memory bank size is 128k and for memory bank ablation study, the temperature is 0.04. All ablations were performed with "Ours-2q" method.

Temperature: The results of varying temperature between 0.02 and 1.0 are shown in Figure 3(a). We find that the optimal temperature is 0.04, and the student gets worse as the temperature gets

Table 5: Linear evaluation on ImageNet and Places: Comparison with SOTA self-supervised methods. We pick the best layer to report the results that is written in parenthesis: 'f7' refers to 'fc7' layer and 'c4' refers to 'conv4' layer. R50x4 refers to the teacher that is trained with SimCLR and R50 to the teacher trained with MoCo. * refers to 10-crop evaluation. † denotes concurrent methods.

Method	Ref	ImageNet top-1	Places top-1		Method	Ref	ImageNet top-1	
AlexNet				ResNet-18				
Sup. on ImageNet	-	56.5 (f7)	39.4 (c4)		Supervised	-	69.8 (L5)	
Inpainting [42]	[60]	21.0 (c3)	23.4 (c3)		InstDisc[57]	[57]	44.5 (L5)	
BiGAN [14]	[38]	29.9 (c4)	31.8 (c3)		LA* [67]	[67]	52.8 (L5)	
Colorization [64]	[19]	31.5 (c4)	30.3 (c4)		MoCo	-	54.5 (L5)	
Context [13]	[19]	31.7 (c4)	32.7 (c4)		Ours-2q (from R50)	-	61.7 (L5)	
Jigsaw [36]	[19]	34.0 (c3)	35.0 (c3)		Ours-1q (from R50)	-	62.6 (L5)	
Counting [37]	[38]	34.3 (c3)	36.3 (c3)	ResNet-50				
SplitBrain [65]	[38]	35.4 (c3)	34.1 (c4)		Resiver	-50		
InstDisc [57]	[57]	35.6 (c5)	34.5 (c4)		Supervised	-	76.2 (L5)	
CC+Vgg+Jigsaw [38]	[38]	37.3 (c3)	37.5 (c3)		InstDisc [57]	[57]	54.0 (L5)	
RotNet [19]	[19]	38.7 (c3)	35.1 (c3)		CF-Jigsaw [58]	[58]	55.2 (L4)	
Artifact [29]	[17]	38.9 (c4)	37.3 (c4)		CF-RotNet [58]	[58]	56.1 (L4)	
AND [28]	[60]	39.7 (c4)	- ` ´		LA * [67]	[67]	60.2 (L5)	
DeepCluster [7]	[7]	39.8 (c4)	37.5 (c4)		SeLa [60]	[60]	61.5 (L5)	
LA* [67]	[67]	42.4 (c5)	40.3 (c4)		PIRL [35]	[35]	63.6 (L5)	
CMC [49]	[60]	42.6 (c5)	- ` ´		SimCLR [9]	[9]	69.3 (L5)	
AET [63]	[60]	44.0 (c3)	37.1 (c3)		MoCo [10]	[10]	71.1 (L5)	
RFDecouple [17]	[17]	44.3 (c5)	38.6 (c5)		InfoMin [†] [51]	[51]	73.0 (L5)	
SeLa+Rot+aug [60]	[60]	44.7 (c5)	37.9 (c4)		BYOL [†] [22]	[22]	74.3 (L5)	
MoCo	-	45.7 (f7)	36.6 (c4)		SwAV [†] [8]	[8]	75.3 (L5)	
Ours-2q (from R50x4)	-	57.6 (f7)	40.4 (c5)		Ours-2q (from R50x4)	-	71.0 (L5)	
Ours-1q (from R50x4)	-	59.0 (f7)	40.3 (c5)		Ours-1q (from R50x4)	-	71.9 (L5)	

ter results on the 1% dataset. This demontuned. * denotes bigger AlexNet [60]. strates that our method can produce more dataefficient models. * denotes concurrent methods.

Method	To	p-1	Top-5		
Method	1%	10%	1%	10%	
Supervised	25.4	56.4	48.4	80.4	
InstDisc [57]	-	-	39.2	77.4	
PIRL [35]	-	-	57.2	83.8	
SimCLR [9]	48.3	65.6	75.5	87.8	
BYOL* [22]	53.2	68.8	78.4	89.0	
SwAV* [8]	53.9	70.2	78.5	89.9	
Only the linear	r layer i	is traine	ed.		
Ours-2q	57.8	66.3	80.4	87.0	
Ours-1q	59.7	67.0	82.3	87.5	

Table 6: Evaluation of ResNet-50 features Table 7: Transferring to PASCAL-VOC classificaon smaller set of ImageNet: ResNet-50x4 is tion and detection tasks: All models use AlexNet used as the teacher. Unlike other methods that and ours is compressed from ResNet-50x4. Our fine-tune the whole network, we only train the model is on par with ImageNet supervised model. last layer. Interestingly, despite fine-tuning For classification, we denote the fine-tuned layers fewer parameters, our method achieves bet- in the parenthesis. For detection, all layers are fine-

Method	Cls.	Det.
	mAP	mAP
Supervised on ImageNet	79.9 (all)	59.1
Random Rescaled [60]	56.6 (all)	45.6
Context* [13]	65.3 (all)	51.1
Jigsaw [36]	67.6 (all)	53.2
Counting [37]	67.7 (all)	51.4
CC+vgg-Jigsaw++ [38]	72.5 (all)	56.5
Rotation [19]	73.0 (all)	54.4
DeepCluster* [7]	73.7 (all)	55.4
RFDecouple* [17]	74.7 (all)	58.0
SeLa+Rot* [60]	77.2 (all)	59.2
MoCo [24]	71.3 (fc8)	55.8
Ours-2q	79.7 (fc8)	58.1
Ours-1q	76.2 (fc8)	59.3

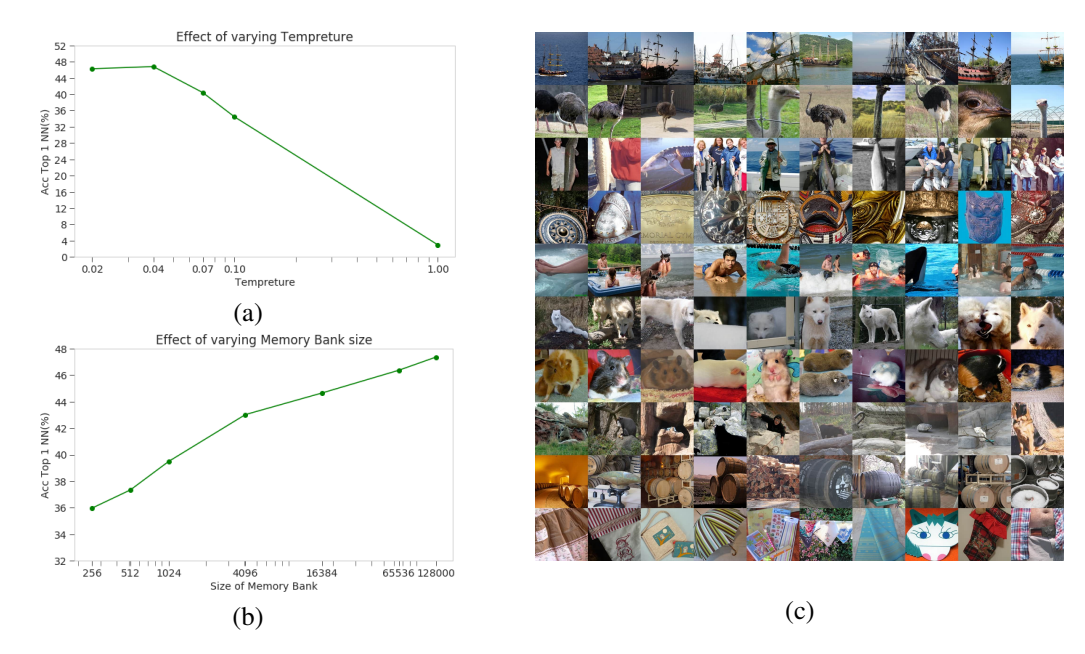


Figure 3: **Ablation and qualitative results:** We show the effect of varying the temperature in (a) and memory bank size in (b) using ResNet-18 distilled from cached features of MoCo ResNet-50. In (c), we show randomly selected images from randomly selected clusters for our best AlexNet model. Each row is a cluster. This is done *without cherry-picking* or manual inspection. Note that most rows are aligned with semantic categories. We have more of these examples in the Appendix.

closer to 1.0. We believe this happens since a small temperature focuses on close neighborhoods by sharpening the probability distribution. A similar behavior is also reported in [9]. As opposed to the other similarity based distillation methods [41, 43, 40, 53], by using small temperature, we focus on the close neighborhood of a data point which results in an improved student.

Size of memory bank: Intuitively, larger number of anchor points should capture more details about the geometry of the teacher's embedding thus resulting in a student that approximates the teacher more closely. We validate this in Figure 3(b) where a larger memory bank results in a more accurate student. When coupled with a small temperature, the large memory bank can help find anchor points that are closer to a query point, thus accurately depicting its close neighborhood.

Effect of momentum parameter: We evaluate various momentum parameters [24] in range (0.999, 0.7, 0.5, 0) and got NN accuracy of (47.35%, 47.45%, 47.40%, 47.34%) respectively. It is interesting that unlike [24], we do not see any reduction in accuracy by removing the momentum. The cause deserves further investigation. Note that momentum is only applicable in case of "ours-2q" method.

Effect of caching the teacher features: We study the effect of caching the feature of the whole training data in compressing ResNet-50 to ResNet-18 using all ImageNet training data. We realize that caching reduces the accuracy by only a small margin 53.4% to 53.0% on NN and 61.7% to 61.2% on linear evaluation while reducing the running time by a factor of almost 3. Hence, for all experiments using ResNet-50x4, we cache the teacher as we cannot afford not doing so.

5 Conclusion

We introduce a simple compression method to train SSL models using deeper SSL teacher models. Our model outperforms the supervised counterpart in the same task of ImageNet classification. This is interesting as the supervised model has access to strictly more information (labels). Obviously, we do not conclude that our SSL method works better than supervised models "in general". We simply compare with the supervised AlexNet that is trained with cross-entropy loss, which is standard in the SSL literature. One can use a more advanced supervised training e.g., compressing supervised ResNet50x4 to AlexNet, to get much better performance for the supervised model.

Acknowledgment: This material is based upon work partially supported by the United States Air Force under Contract No. FA8750-19-C-0098, funding from SAP SE, and also NSF grant number 1845216. Any opinions, findings, and conclusions or recommendations expressed in this material are those of the authors and do not necessarily reflect the views of the United States Air Force, DARPA, and other funding agencies. Moreover, we would like to thank Vipin Pillai and Erfan Noury for the valuable initial discussions. We also acknowledge the fruitful comments by all reviewers specifically by Reviewer 2 for suggesting to use teacher's queue for the student, which improved our results.

Broader Impact

Ethical concerns of AI: Most AI algorithms can be exploited for non-ethical applications. Unfortunately, our method is not an exception. For instance, rich self-supervised features may enable harmful surveillance applications.

AI for all: Model compression reduces the computation needed in inference and self-supervised learning reduces annotation needed in training. Both these benefits may make rich deep models accessible to larger community that do not have access to expensive computation and labeling resources.

Privacy and edge computation: Model compression enables running deep models on the devices with limited computational and power resources e.g., IoT devices. This reduces the privacy issues since the data does not need to be uploaded to the cloud. Moreover, compressing self-supervised learning models can be even better in this sense since a small model e.g., MobileNet that generalizes to new tasks well, can be finetuned on the device itself, so even the finetuning data does not need to be uploaded to the cloud.

References

- [1] A library for efficient similarity search and clustering of dense vectors. https://github.com/facebookresearch/faiss.
- [2] Sungsoo Ahn et al. "Variational information distillation for knowledge transfer." In: Proceedings of the IEEE Conference on Computer Vision and Pattern Recognition. 2019, pp. 9163–9171.
- [3] Jimmy Ba and Rich Caruana. "Do deep nets really need to be deep?" In: *Advances in neural information processing systems*. 2014, pp. 2654–2662.
- [4] Philip Bachman, R Devon Hjelm, and William Buchwalter. "Learning representations by maximizing mutual information across views." In: *Advances in Neural Information Processing Systems*. 2019, pp. 15509–15519.
- [5] Hessam Bagherinezhad et al. "Label refinery: Improving imagenet classification through label progression." In: *arXiv preprint arXiv:1805.02641* (2018).
- [6] Cristian Buciluă, Rich Caruana, and Alexandru Niculescu-Mizil. "Model compression." In: *Proceedings of the 12th ACM SIGKDD international conference on Knowledge discovery and data mining*. 2006, pp. 535–541.
- [7] Mathilde Caron et al. "Deep clustering for unsupervised learning of visual features." In: *Proceedings of the European Conference on Computer Vision (ECCV)*. 2018, pp. 132–149.
- [8] Mathilde Caron et al. "Unsupervised learning of visual features by contrasting cluster assignments." In: *arXiv preprint arXiv:2006.09882* (2020).
- [9] Ting Chen et al. "A Simple Framework for Contrastive Learning of Visual Representations." In: *arXiv preprint arXiv:2002.05709* (2020).
- [10] Xinlei Chen et al. "Improved Baselines with Momentum Contrastive Learning." In: *arXiv* preprint arXiv:2003.04297 (2020).
- [11] Contrastive Multiview Coding. https://github.com/HobbitLong/CMC.
- [12] Contrastive Representation Distillation (CRD), and benchmark of recent knowledge distillation methods. https://github.com/HobbitLong/RepDistiller.
- [13] Carl Doersch, Abhinav Gupta, and Alexei A Efros. "Unsupervised visual representation learning by context prediction." In: *Proceedings of the IEEE International Conference on Computer Vision*. 2015, pp. 1422–1430.

- [14] Jeff Donahue, Philipp Krähenbühl, and Trevor Darrell. "Adversarial feature learning." In: *International Conference on Learning Representations, ICLR*. 2016.
- [15] Alexey Dosovitskiy et al. "Discriminative unsupervised feature learning with convolutional neural networks." In: *Advances in neural information processing systems*. 2014, pp. 766–774.
- [16] Mark Everingham et al. "The pascal visual object classes (voc) challenge." In: *International journal of computer vision* 88.2 (2010), pp. 303–338.
- [17] Zeyu Feng, Chang Xu, and Dacheng Tao. "Self-supervised representation learning by rotation feature decoupling." In: *Proceedings of the IEEE Conference on Computer Vision and Pattern Recognition*. 2019, pp. 10364–10374.
- [18] Tommaso Furlanello et al. "Born-Again Neural Networks." In: *Proceedings of the 35th International Conference on Machine Learning, ICML 2018, Stockholmsmässan, Stockholm, Sweden, July 10-15, 2018.* Ed. by Jennifer G. Dy and Andreas Krause. Vol. 80. Proceedings of Machine Learning Research. PMLR, 2018, pp. 1602–1611. URL: http://proceedings.mlr.press/v80/furlanello18a.html.
- [19] Spyros Gidaris, Praveer Singh, and Nikos Komodakis. "Unsupervised Representation Learning by Predicting Image Rotations." In: *International Conference on Learning Representations*. 2018. URL: https://openreview.net/forum?id=S1v4N2l0-.
- [20] Ross Girshick. "Fast r-cnn." In: *Proceedings of the IEEE international conference on computer vision*. 2015, pp. 1440–1448.
- [21] Priya Goyal et al. "Scaling and benchmarking self-supervised visual representation learning." In: Proceedings of the IEEE International Conference on Computer Vision. 2019, pp. 6391–6400.
- [22] Jean-Bastien Grill et al. "Bootstrap your own latent: A new approach to self-supervised learning." In: *arXiv preprint arXiv:2006.07733* (2020).
- [23] Raia Hadsell, Sumit Chopra, and Yann LeCun. "Dimensionality reduction by learning an invariant mapping." In: 2006 IEEE Computer Society Conference on Computer Vision and Pattern Recognition (CVPR'06). Vol. 2. IEEE. 2006, pp. 1735–1742.
- [24] Kaiming He et al. "Momentum contrast for unsupervised visual representation learning." In: *Proceedings of the IEEE/CVF Conference on Computer Vision and Pattern Recognition*. 2020, pp. 9729–9738.
- [25] Olivier J Hénaff et al. "Data-efficient image recognition with contrastive predictive coding." In: arXiv preprint arXiv:1905.09272 (2019).
- [26] Geoffrey Hinton, Oriol Vinyals, and Jeff Dean. "Distilling the knowledge in a neural network." In: *arXiv preprint arXiv:1503.02531* (2015).
- [27] R Devon Hjelm et al. "Learning deep representations by mutual information estimation and maximization." In: *International Conference on Learning Representations*. 2019. URL: https://openreview.net/forum?id=Bklr3j0cKX.
- [28] Jiabo Huang et al. "Unsupervised Deep Learning by Neighbourhood Discovery." In: ed. by Kamalika Chaudhuri and Ruslan Salakhutdinov. Vol. 97. Proceedings of Machine Learning Research. Long Beach, California, USA: PMLR, Sept. 2019, pp. 2849–2858. URL: http://proceedings.mlr.press/v97/huang19b.html.
- [29] Simon Jenni and Paolo Favaro. "Self-supervised feature learning by learning to spot artifacts." In: Proceedings of the IEEE Conference on Computer Vision and Pattern Recognition. 2018, pp. 2733–2742.
- [30] Xu Ji, João F Henriques, and Andrea Vedaldi. "Invariant information clustering for unsupervised image classification and segmentation." In: *Proceedings of the IEEE International Conference on Computer Vision*. 2019, pp. 9865–9874.
- [31] Jangho Kim, SeongUk Park, and Nojun Kwak. "Paraphrasing complex network: Network compression via factor transfer." In: *Advances in Neural Information Processing Systems*. 2018, pp. 2760–2769.
- [32] Jonathan Krause et al. "3d object representations for fine-grained categorization." In: Proceedings of the IEEE international conference on computer vision workshops. 2013, pp. 554–561.
- [33] Harold W Kuhn. "The Hungarian method for the assignment problem." In: *Naval research logistics quarterly* 2.1-2 (1955), pp. 83–97.

- [34] Tomasz Malisiewicz, Abhinav Gupta, and Alexei A Efros. "Ensemble of exemplar-syms for object detection and beyond." In: 2011 International conference on computer vision. IEEE. 2011, pp. 89–96.
- [35] Ishan Misra and Laurens van der Maaten. "Self-supervised learning of pretext-invariant representations." In: *arXiv preprint arXiv:1912.01991* (2019).
- [36] Mehdi Noroozi and Paolo Favaro. "Unsupervised learning of visual representations by solving jigsaw puzzles." In: *European Conference on Computer Vision*. Springer. 2016, pp. 69–84.
- [37] Mehdi Noroozi, Hamed Pirsiavash, and Paolo Favaro. "Representation learning by learning to count." In: *Proceedings of the IEEE International Conference on Computer Vision*. 2017, pp. 5898–5906.
- [38] Mehdi Noroozi et al. "Boosting self-supervised learning via knowledge transfer." In: Proceedings of the IEEE Conference on Computer Vision and Pattern Recognition. 2018, pp. 9359–9367.
- [39] Aaron van den Oord, Yazhe Li, and Oriol Vinyals. *Representation Learning with Contrastive Predictive Coding*. 2018. arXiv: 1807.03748 [cs.LG].
- [40] Wonpyo Park et al. "Relational knowledge distillation." In: *Proceedings of the IEEE Conference on Computer Vision and Pattern Recognition*. 2019, pp. 3967–3976.
- [41] Nikolaos Passalis and Anastasios Tefas. "Learning deep representations with probabilistic knowledge transfer." In: *Proceedings of the European Conference on Computer Vision (ECCV)*. 2018, pp. 268–284.
- [42] Deepak Pathak et al. "Context encoders: Feature learning by inpainting." In: *Proceedings of the IEEE conference on computer vision and pattern recognition*. 2016, pp. 2536–2544.
- [43] Baoyun Peng et al. "Correlation congruence for knowledge distillation." In: *Proceedings of the IEEE International Conference on Computer Vision*. 2019, pp. 5007–5016.
- [44] PyTorch implementation of MoCo: https://arxiv.org/abs/1911.05722. https://github.com/facebookresearch/moco.
- [45] Adriana Romero et al. "FitNets: Hints for Thin Deep Nets." In: 3rd International Conference on Learning Representations, ICLR 2015, San Diego, CA, USA, May 7-9, 2015, Conference Track Proceedings. Ed. by Yoshua Bengio and Yann LeCun. 2015. URL: http://arxiv.org/abs/1412.6550.
- [46] Olga Russakovsky et al. "ImageNet Large Scale Visual Recognition Challenge." In: *International Journal of Computer Vision (IJCV)* 115.3 (2015), pp. 211–252. DOI: 10.1007/s11263-015-0816-y.
- [47] SimCLR A Simple Framework for Contrastive Learning of Visual Representations https://arxiv.org/abs/2002.05709. https://github.com/google-research/simclr.
- [48] Antti Tarvainen and Harri Valpola. "Mean teachers are better role models: Weight-averaged consistency targets improve semi-supervised deep learning results." In: *Advances in neural information processing systems*. 2017, pp. 1195–1204.
- [49] Yonglong Tian, Dilip Krishnan, and Phillip Isola. "Contrastive multiview coding." In: *arXiv* preprint arXiv:1906.05849 (2019).
- [50] Yonglong Tian, Dilip Krishnan, and Phillip Isola. "Contrastive Representation Distillation." In: *International Conference on Learning Representations*. 2020. URL: https://openreview.net/forum?id=SkgpBJrtvS.
- [51] Yonglong Tian et al. "What makes for good views for contrastive learning." In: *arXiv preprint arXiv:2005.10243* (2020).
- [52] Torchvision Models. https://pytorch.org/docs/stable/torchvision/ models.html.
- [53] Frederick Tung and Greg Mori. "Similarity-preserving knowledge distillation." In: *Proceedings of the IEEE International Conference on Computer Vision*. 2019, pp. 1365–1374.
- [54] Unsupervised Learning of Visual Features by Contrasting Cluster Assignments. https://github.com/facebookresearch/swav.
- [55] Peter Welinder et al. "Caltech-UCSD birds 200." In: (2010).
- [56] Ancong Wu et al. "Distilled Person Re-Identification: Towards a More Scalable System." In: *The IEEE Conference on Computer Vision and Pattern Recognition (CVPR)*. June 2019.

- [57] Zhirong Wu et al. "Unsupervised feature learning via non-parametric instance discrimination." In: *Proceedings of the IEEE Conference on Computer Vision and Pattern Recognition*. 2018, pp. 3733–3742.
- [58] Xueting Yan et al. "ClusterFit: Improving Generalization of Visual Representations." In: CVPR. 2020.
- [59] Junho Yim et al. "A gift from knowledge distillation: Fast optimization, network minimization and transfer learning." In: *Proceedings of the IEEE Conference on Computer Vision and Pattern Recognition*. 2017, pp. 4133–4141.
- Asano YM., Rupprecht C., and Vedaldi A. "Self-labelling via simultaneous clustering and representation learning." In: *International Conference on Learning Representations*. 2020. URL: https://openreview.net/forum?id=Hyx-jyBFPr.
- [61] Lu Yu et al. "Learning Metrics From Teachers: Compact Networks for Image Embedding." In: *The IEEE Conference on Computer Vision and Pattern Recognition (CVPR)*. June 2019.
- [62] Sergey Zagoruyko and Nikos Komodakis. "Paying More Attention to Attention: Improving the Performance of Convolutional Neural Networks via Attention Transfer." In: *ICLR*. 2017. URL: https://arxiv.org/abs/1612.03928.
- [63] Liheng Zhang et al. "Aet vs. aed: Unsupervised representation learning by auto-encoding transformations rather than data." In: *Proceedings of the IEEE Conference on Computer Vision and Pattern Recognition*. 2019, pp. 2547–2555.
- [64] Richard Zhang, Phillip Isola, and Alexei A Efros. "Colorful image colorization." In: *European conference on computer vision*. Springer. 2016, pp. 649–666.
- [65] Richard Zhang, Phillip Isola, and Alexei A Efros. "Split-brain autoencoders: Unsupervised learning by cross-channel prediction." In: *Proceedings of the IEEE Conference on Computer Vision and Pattern Recognition*. 2017, pp. 1058–1067.
- [66] Bolei Zhou et al. "Learning deep features for scene recognition using places database." In: *Advances in neural information processing systems*. 2014, pp. 487–495.
- [67] Chengxu Zhuang, Alex Lin Zhai, and Daniel Yamins. "Local aggregation for unsupervised learning of visual embeddings." In: *Proceedings of the IEEE International Conference on Computer Vision*. 2019, pp. 6002–6012.

Appendix

Table A1: **Parameter and FLOPs comparison:** We report the number of floating point operations (FLOPs) and the number of parameters in a model below.

Model	FLOPs (G)	Params (M)
MobileNet-V2	0.33	3.50
AlexNet	0.77	61.0
ResNet-18	1.82	11.69
ResNet-50	4.14	25.56
ResNet-50x4	64.06	375.38

More results for cluster alignment

For cluster alignment experiment (Section 4.3), we calculate the alignment for each category, sort them, and show in Figure A1. Moreover, Figure A2 is a larger version that is generated similar to Figure 3-right. Each row is a random cluster while images in the row are randomly sampled from that cluster with no manual selection or cherry-picking.

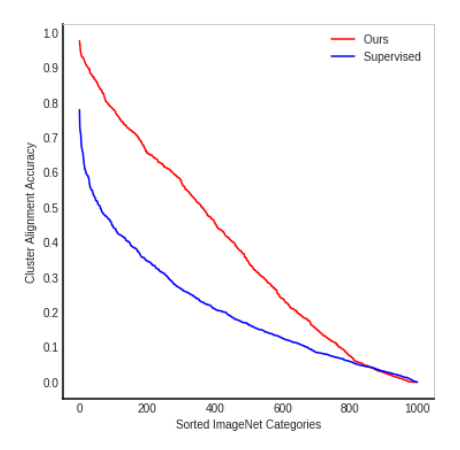


Figure A1: **Cluster alignment accuracy:** We calculate the accuracy for each ImageNet category and then plot them after sorting.

Implementation details for the baselines

Non-compressed (MoCo): We use MoCo-v2 [10] from the official code [44] with AlexNet, ResNet-18, and MobileNet-V2 architectures for 200 epochs. We also train a longer baseline with ResNet-18 for 1000 epochs. All other hyperparameters are the same as the official version (m=0.999, lr=0.03).

CRD: We use the official code provided by the authors[12] and removed the supervised loss term. We use their default ImageNet hyperparameter of lr=0.05 except for AlexNet student for which we use lr=0.005 to make it converge.

CC: We calculate the ℓ_2 normalized embeddings for the entire training dataset and apply k-means clustering with (k=16,000) (which is adopted from [58]). This is equivalent to clustering with cosine similarity. We got slightly better results for cosine similarity compared to Euclidean distance. We use the FAISS GPU based k-means clustering implementation[1]. Finally, the student is trained to classify the cluster assignments. As in [38, 58], we train the student for 100 epochs. We use lr=0.1 for ResNet models and lr=0.01 for MobileNet-V2 and AlexNet models. We use cosine learning rate annealing.

Reg: We use Adam optimizer with weight decay of 1e - 4 for 100 epochs, and batch size of 256. For MobileNet-V2 and ResNet-18, we use lr = 0.001, and for AlexNet lr = 0.0001. The lr is reduced

by a factor of 10 at the 40-th and 80-th epochs. We use ADAM optimizer as performed better than SGD.

Reg-BN: It is similar to Reg except that we use SGD optimizer with lr = 0.1 instead of ADAM.

Details of Places experiments (Section 4.4)

We perform adaptive max pooling to get features with dimensions around 9K, and train a linear layer on top of them. Training is done for 90 epochs with lr = 0.01, batch size = 256, weight decay = 1e - 4, momentum = 0.9, and lr multiplied by 0.1 at 30, 60, and 80 epochs.

Details of PASCAL experiments (Section 4.4)

For classification, we train a single linear layer on top of a frozen backbone. We use SGD with learning rate = 0.01, batch size = 16, weight decay = 1e-6, and momentum = 0.9. We train for 80,000 iterations and multiply learning rate by 0.5 every 5,000 iterations.

For object detection, we use SGD learning rate = 0.001, weight decay = 5e - 4, momentum = 0.9 and batch size = 256. We train for 15,000 iterations and multiply learning rate by 0.1 every 5,000 iterations. The training parameters are adopted form [38] and the code from [20].

Details of small data ImageNet experiments (Section 4.4)

We train a single linear layer on top a frozen backbone. We use SGD with learning rate = 0.05, batch size = 256, weight decay = 1e - 4, and momentum = 0.9. We use cosine learning rate decay and train for 30 and 60 epochs for 10 percent and 1 percent subsets respectively. The subsets and training parameters are adopted from [9].



Figure A2: **Cluster Alignment:** Similar to Figure 3 (c), we show 20 randomly selected images (columns) from 30 randomly selected clusters (rows) for our best AlexNet modal. This is done with no manual inspection or cherry-picking. Note that most rows are aligned with semantic categories.